

GT-2002-30630

**EVALUATING ENVIRONMENTAL BARRIER COATINGS ON CERAMIC MATRIX COMPOSITES
AFTER ENGINE AND LABORATORY EXPOSURES**

Karren L. More, Peter F. Tortorelli, and Larry R. Walker
Oak Ridge National Laboratory, Oak Ridge, Tennessee

Josh B. Kimmel, Narendernath Miriyala, and Jeffrey R. Price
Solar Turbines Inc., San Diego, California

Harry E. Eaton, Ellen Y. Sun, and Gary D. Linsey
United Technologies Research Center, East Hartford, CT

ABSTRACT

SiC/SiC continuous fiber-reinforced ceramic matrix composite (CFCC) combustor liners having protective environmental barrier coatings (EBCs) applied to the liner working surfaces have been field-tested in a Solar Turbines' Centaur 50S SoLoNOx engine at the Chevron, Bakersfield, CA engine test site. This latest engine test ran for a total of 13,937h. The EBCs significantly increased the lifetime of the in-service liners compared with uncoated CFCC liners used in previous field-tests. The engine test was concluded when a routine borescope inspection revealed the formation of a small hole in the inner liner. Extensive microstructural evaluation of both the inner and outer liners was conducted after removal from the engine. Post-test analysis indicated that numerous degradation mechanisms contributed to the EBC and CFCC damage observed on the liners, including EBC volatilization, sub-surface CFCC oxidation and recession, and processing defects which resulted in localized EBC spallation and accelerated CFCC oxidation. The characterization results obtained from these field-tested liners have been compared with the analyses of similarly-processed CFCC/EBCs that were laboratory-tested in a high-pressure, high temperature exposure facility (the ORNL "Keiser Rig") for >6000h.

INTRODUCTION

Over the past four years, several continuous fiber-reinforced ceramic composite (CFCC) combustor liners have been field-tested in a Solar Turbines' Centaur 50S SoLoNOx engine at the Chevron, Bakersfield, CA site (formerly Texaco) as part of DOE's Ceramics for Stationary Gas Turbines (CSGT) Program. The first four field tests were conducted using uncoated SiC/SiC CFCC inner and outer liners,

with improvements made to the CFCC after each test to prolong the liner life.[1-3] These improvements included the utilization of high temperature fibers, different matrix compositions, and protective SiC seal coats on the liner surfaces. After engine testing, microstructural evaluation was conducted on the liners to measure surface recession rates and understand degradation mechanisms for the different CFCC liners.[4,5] Excessive composite damage was observed on the liners after each of the first four engine tests and high surface recession rates were measured for the SiC/SiC liner materials. It has been shown that exposure of Si-based materials to the high water-vapor pressures (>1atm) typical of gas turbine combustion environments results in rapid oxidation [6,7] and surface recession due to SiO₂ volatilization.[8,9]

To increase the lifetimes of CFCC combustor liners to >30,000h, as required by gas turbine manufacturers and end users, protective surface coatings will be necessary. These coatings must prevent the diffusion of oxidants to the underlying CFCC material and be resistant to volatilization in the combustion environment. To this end, environmental barrier coating (EBC) systems have been evaluated for use on CFCC combustor liners.[10,11] The oxide-based EBCs currently being evaluated for use on CFCC liners are based on a coating system developed initially under NASA's High Speed Civil Transport (HSCT) and Enabling Propulsion Materials (EPM) Programs [10,12] and have been optimized and scaled-up under the current DOE CSGT Program for the gas turbine combustor liner application. These EBCs showed positive results when laboratory-tested in the high water vapor pressures and intermediate gas velocities typical of gas turbine combustion environments and have successfully been applied to actual CFCC liners.

In the present study, inner and outer EBC/CFCC liners ran in a

recent Chevron engine test for ~13,937h, significantly increasing the lifetime of the in-service liners compared with uncoated CFCC liners used in all four of the previous field-tests. Extensive microstructural characterization was conducted following this engine test in order to understand degradation mechanisms contributing to the observed EBC damage on the liner working surfaces that accumulated during field-testing. In addition, long-term laboratory-scale exposures in a high temperature, high pressure exposure facility (the Keiser Rig) have been conducted to complement the engine exposures of similarly-processed EBC/CFCC systems.

EXPERIMENTAL BACKGROUND

Both CFCC liners used in the fifth Chevron engine-test were manufactured by GE Power Systems Composites (formerly Honeywell Advanced Composites, Inc.) The 33cm diameter inner liner was produced using the Si-melt infiltration (MI) process and consisted of continuous (wound) Hi-Nicalon SiC fibers with a BN interfacial coating in a dense Si+SiC matrix. The 76cm diameter outer liner was fabricated by the chemical vapor infiltration (CVI) process and was fabricated using wound Hi-Nicalon SiC fibers having a pyrolytic carbon interfacial coating in a CVI SiC matrix. Microstructural differences between the MI and CVI CFCC materials are summarized in Ref. 7. Each liner also had a protective SiC seal coat applied by chemical vapor deposition (CVD) which was ~440 μ m thick on the MI inner liner and ~520 μ m thick on the CVI outer liner.

The fifth Chevron field-test was the first engine test with EBC protection on the CFCC liners.[10] Two different air plasma sprayed EBCs were used on the liners. The inner liner had a three layer "standard" EBC system consisting of a ~125 μ m Si bond coat, a ~125 μ m mullite intermediate layer, and a ~125 μ m Ba_{0.75}Sr_{0.25}Al₂Si₂O₈ (BSAS) top coat, as shown in Fig. 1. The outer liner also had a three layer EBC system, except in this case the intermediate layer was a mixed-layer of mullite+BSAS, as shown in Fig. 2.

The engine test, started in April, 1999, was stopped in November, 2000 after a small hole was observed on the inner liner during a routine borescope inspection. The engine test ran for a total of ~14,000h. Additional details of the combustor liner design and fifth engine test are given in Ref. 13. After the liners were removed from the engine, each was sent to Argonne National Laboratory for nondestructive evaluation (NDE) and comparison with similar data acquired on the liners before engine testing.[13] Visual inspection of the liners showed areas with varying degrees of surface damage. Typical surface areas observed are shown in Fig. 3a-c. The most severe areas of localized damage on both the inner and outer liner working surfaces corresponded with the fuel injector impingement areas (Fig. 3a) where the EBC was completely gone. Many other areas on both liners showed the EBC fully intact or having minimal surface damage (Fig. 3b). A pattern of "pinhole" damage was evident on both liners, but was most prevalent on the outer liner (Fig. 3c). Other types of damage observed, i.e., areas where edge spallation was evident and areas where the EBC spalled off in the early stages of the engine test (NDE results indicated that these early-spall areas were possibly due to a CVD SiC seal coat delamination) are summarized elsewhere.[11,13]

Since there were so many areas showing different types of EBC damage, an extensive microstructural evaluation of the different damaged areas on each liner was undertaken. Eight carefully selected large sections were laser-cut from each liner and subsequently cut into

2.54cm wide strips. The strips were distributed among the various program participants, Oak Ridge National Laboratory (ORNL), United Technologies Research Center, Argonne National Laboratory, and Solar Turbines, Inc. in order for each participant to conduct in-house analysis. This paper presents the results of extensive microstructural characterization performed at ORNL. Other analyses, including mechanical properties evaluation, will be presented elsewhere.

Laboratory exposures were conducted in ORNL's Keiser Rig for the first-stage evaluation of the two types of EBCs used on the CFCC combustor liners in the fifth Chevron engine test. The ORNL rig has been described in detail previously.[4,14] In order to best simulate the combustor environment of the Solar Turbines Centaur 50S engine, all Keiser Rig exposures were conducted at 1204°C (2200°F), 1.5atm H₂O (balance air), and 10atm total system pressure. Each exposure was run for 500h, after which the specimens were carefully removed and sectioned for microstructural analysis. The specimens were then placed back in the furnace for additional exposure under the same conditions. A total of 6500h was accumulated on the EBC/CFCC (MI) coupons for comparison with the similarly-processed EBC/CFCC engine-tested combustor liners.

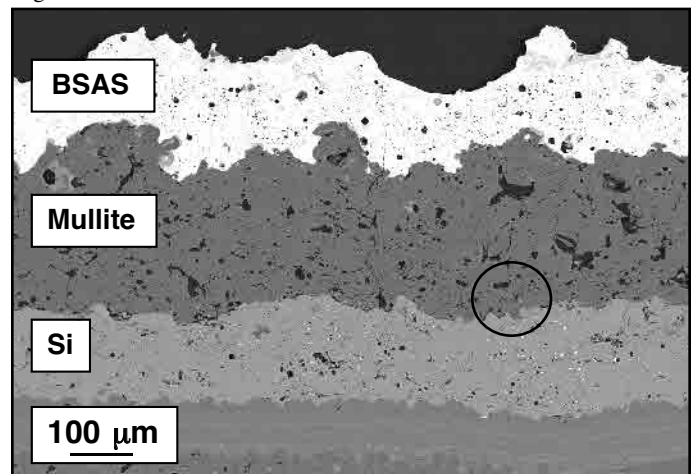


Fig. 1. Typical as-processed microstructure of three layer EBC having a mullite intermediate layer.

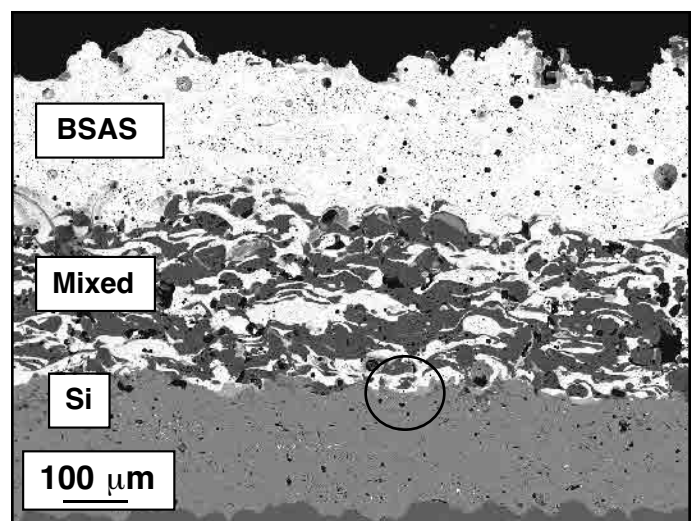


Fig. 2. Typical as-processed microstructure of three layer EBC with "mixed" (mullite+BSAS) intermediate layer.

RESULTS AND DISCUSSION

ORNL Laboratory Exposures of Representative EBCs

Much of the work prior to EBC down-selection for the fifth Chevron engine test focused on exposing numerous experimental EBCs to the high water-vapor pressures typically encountered during combustion in a gas turbine engine. Initial results of these early exposures coupled with microstructural characterization were used to improve the processing of the coatings to reduce or prevent the formation of excess through-thickness cracks and large-scale porosity and to evaluate uniformity of the coatings once scale-up for EBC application on actual liners was achieved. The EBC/CFCC coupons of the two representative coatings (see Fig. 1 and 2) prepared for exposure in the Keiser Rig were processed in a manner similar to the final processing conditions used for the actual combustor liners. The two EBCs were exposed simultaneously using the Keiser Rig conditions given in Experimental Background.

In order to provide the necessary protection for the underlying composite, the EBC must be an effective diffusion barrier to oxidation (primarily H_2O), be thermally stable, and must also be volatilization-resistant in the combustion environment. Gas velocity (in addition to temperature and H_2O pressure) plays a key role in the volatilization of silica.[8,9] The Keiser Rig is a slow gas-flow system and is not an effective test to evaluate EBC volatilization.[6] However, the Keiser Rig is ideally suited for evaluating the protective capability of EBCs at elevated temperatures and water-vapor pressures. Oxidation damage that accumulates below the EBC due to diffusion of oxidants through the coating is not affected by the gas velocity on the EBC surface. Thus, by viewing the EBC/CFCC in cross-section, the amount and rate of oxidation occurring below the different EBCs can be compared.

With this in mind, differences in the protective capability of each of the two EBCs became apparent in the early stages of exposure in the Keiser Rig. After 1500h at $1200^\circ C$ and 1.5atm H_2O , imaging the Si/mullite (area circled in Fig. 1) or the Si/(mullite+BSAS) (area circled in Fig. 2) interfaces of the EBC revealed oxidation of the Si bond coat which resulted in the formation of SiO_2 at the interfaces during exposure. Differences between the amount of SiO_2 formed after 1500h for the two EBC formulations are shown in Fig. 4 and Fig. 5 for the Si/mullite/BSAS and Si/(mullite+BSAS)/BSAS mixed-layer EBCs, respectively. Note that the amount of SiO_2 formed in the Si/Mullite/BSAS EBC (Fig. 4) was $\sim 5X$ thicker than that formed in the mixed-layer EBC (Fig. 5) indicating that the protective capability of the mixed-layer EBC was superior. In fact, exposure of the Si/mullite/BSAS EBC/CFCC coupon in the Keiser Rig was suspended after 3000h because excessive oxide formation at the Si/mullite interface led to some EBC spallation at this interface. The primary reason for the greater degree of oxidation for the Si/mullite/BSAS EBC is attributed to excessive micro-cracking and porosity within the mullite intermediate layer after EBC processing. The (mullite+BSAS) intermediate layer in the mixed-layer EBC did not show excessive micro-cracking in the as-processed condition. Exposure of the mixed-layer EBC/CFCC coupon was continued for a total exposure time of 6500h. The Si/(mullite+BSAS) interface in the mixed-layer EBC/CFCC after 5000h at $1200^\circ C$ and 1.5atm H_2O is shown in Fig. 6. A comparison of Fig. 5 and Fig. 6 shows only slow thickening of the SiO_2 at extended times, further demonstrating the superiority of this EBC compared to the Si/mullite/BSAS EBC.



Fig. 3a. Severely damaged area on working surface of inner liner corresponding to a typical fuel injector impingement area.



Fig. 3b. Area on working surface of inner liner where EBC appeared to be intact or only slightly damaged.



Fig. 3c. "Pinhole" pattern observed on working surface of outer liner.

The EBC processing parameters were adjusted in the early stages of this work to minimize the number of processing defects (such as through-thickness cracks) on the final EBC/CFCC liners. However, even under the best processing conditions, some processing defects were still found. When these defects were present, accelerated localized oxidation below the EBC was observed, as shown in Fig. 7. Silica formation (Si oxidation) was excessive in these areas.

The results of the Keiser Rig exposures clearly showed that the Si/(mullite+BSAS)/BSAS mixed-layer EBC was superior to that of the Si/mullite/BSAS EBC. However, the exposures were not completed before the decision had to be made regarding the particular EBC to be used for the Chevron engine test. Thus, it was decided to engine-test the viability of each type of EBC. The standard EBC was applied to the MI inner liner and the mixed-layer EBC was applied to the outer liner. In this way, both types of EBCs could be evaluated following the engine test. For later engine tests conducted at the Chevron and Malden Mills test sites, only the mixed-layer EBC was used for both the inner and outer liners.[13]

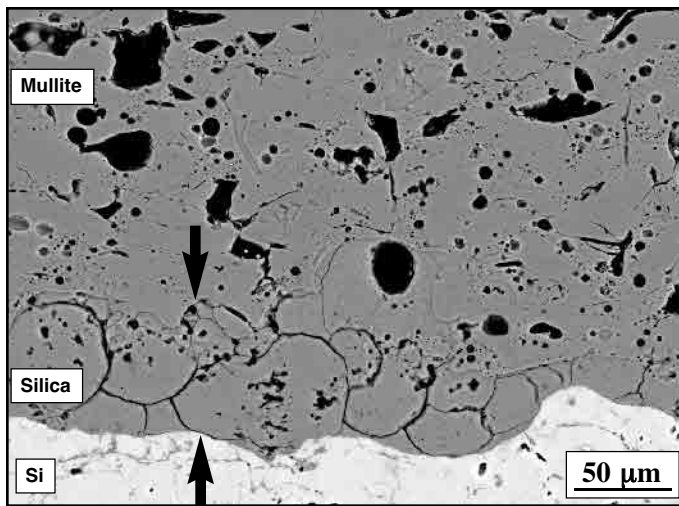


Fig. 4. SEM image of SiO_2 formed at Si/mullite interface ($\sim 50\mu\text{m}$ thick) in standard 3-layer EBC after 1500h at 1200°C and $1.5\text{atm H}_2\text{O}$.

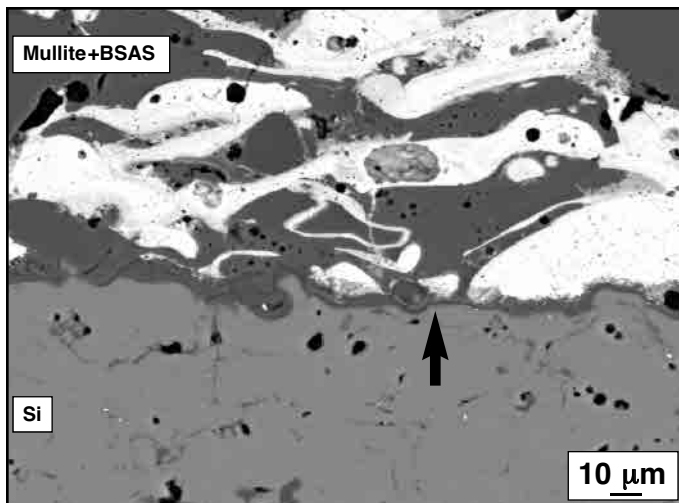


Fig. 5. SEM image of SiO_2 formed at Si/(mullite+BSAS) interface ($<10\mu\text{m}$) in mixed-layer EBC after 1500h at 1200°C and $1.5\text{atm H}_2\text{O}$.

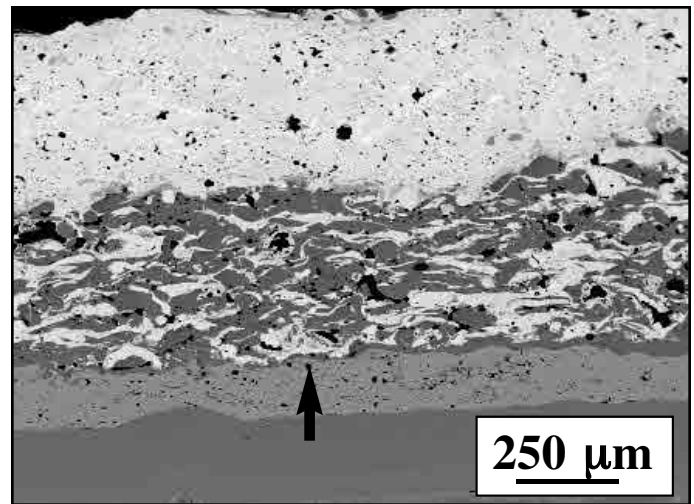


Fig. 6. SEM image of SiO_2 formed at Si/(mullite+BSAS) interface ($\sim 20\mu\text{m}$) in mixed-layer EBC after 5000h at 1200°C and $1.5\text{atm H}_2\text{O}$.

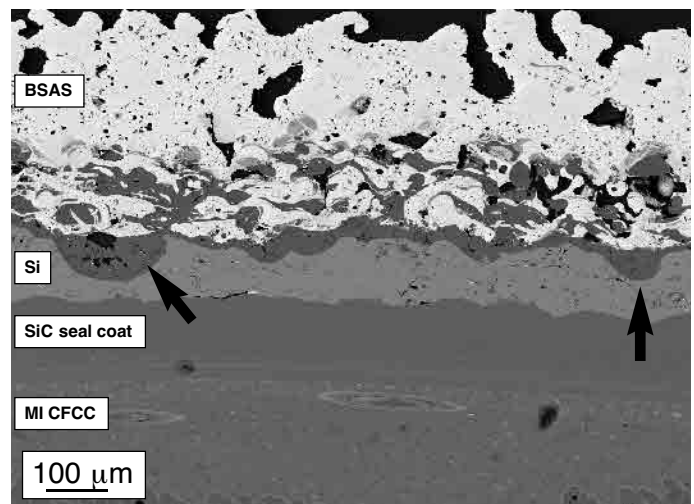


Fig. 7. SEM image of accelerated SiO_2 formation associated with processing defects (excess porosity) in mixed-layer EBC after 5000h at 1200°C and $1.5\text{atm H}_2\text{O}$.

Evaluation of EBC/CFCC Engine Tested Combustor Liners

The EBCs offered significant protection for both the inner and outer CFCC liners used in the fifth Chevron engine test considering both liners lasted 13,937h with most of the surfaces fully intact. Without an EBC applied to the liner working surfaces, the projected lifetimes (100% consumption or material recession) for the CVD SiC seal-coated CFCC liners are as follows:

0.25cm MI inner liner + $440\mu\text{m}$ CVD SiC seal coat = $\sim 10,000\text{h}$

0.25cm CVI outer liner + $520\mu\text{m}$ CVD SiC seal coat = $\sim 8000\text{h}$

Calculations were based on recession rates determined for previously engine-tested uncoated CFCC liners.[7]

In order to evaluate the characteristics of the EBC and CFCC damage accumulated during engine testing, cross-section samples were prepared (from the 2.54cm strips) through the various types of surface damage observed (see Fig. 3a-c). Four primary types of damage were deemed critical after viewing many samples from both

liners (these results do not include EBC areas that were clearly spalled early in the engine test or those associated with the liner edges.) The primary issues, or liner degradation mechanisms, were (1) BSAS volatility in the gas turbine combustion environment, (2) the stability of mullite, (3) oxidation of non-oxide constituents below the EBC, and (4) the contribution of surface asperities to EBC spallation (formation of pinhole defects.) Microstructural evidence for the critical degradation mechanism will be presented and described in detail below.

BSAS Volatility in Combustion Environment. Specimens were prepared from many EBC areas on both liner surfaces where the EBC appeared fully intact (see Fig. 3b.) Figures 8a and 8b, comparing cross-section SEM images of the Si/mullite/BSAS EBC from the aft end of the inner liner and from an area towards its center, respectively, clearly show a significant loss of the BSAS top coat in the center area of the inner liner. Visual inspection of the liner did not provide any information regarding loss of EBC (BSAS). Figures 9a and 9b show a similar comparison for areas of the outer liner. Varying amounts of BSAS loss via volatilization were measured across the inner and outer liner working surfaces. In general, the thickness of the BSAS reduced gradually from the fore end of the liner, which was close to the original as-processed thickness, towards the liner center and then gradually increased again towards the aft end of the liner. (Note that the top layers of the EBC within ~2cm of the aft end of both the inner and outer liners had spalled off due to mechanical problems with the metallic attachment, which has since been redesigned to avoid the problem.[13]) The different amounts of BSAS recession across the surfaces of the liners can be attributed to temperature variations from the cooler ends of the liners to the center and across the center region of both liners (accurate temperature measurements could not be made on the liners during engine testing but were between 1100-1250°C.)

In areas directly associated with fuel injector impingement (Fig. 3a), corresponding to the hottest areas on the liner surfaces, the loss of EBC due to volatilization was extreme. In fact, most of these localized areas showed evidence of gradual surface recession of the EBC down to the CVD SiC seal coat, which had started to oxidize. In two of the fuel injector impingement areas where the EBC had fully volatilized, oxidation of the CFCC material was evident.

A high magnification SEM image of the surface of the BSAS which had experienced some volatilization is shown in Figure 10. A residual phase was observed on the surface which was clearly more resistant to volatilization (brightly imaging phase on surface.) This phase, a Sr-rich phase identified as $\text{Sr}_2\text{Al}_2\text{SiO}_7$ by X-ray diffraction, remained on the surface of the top coat longer than the BSAS. This phase has its origins in the as-processed BSAS top coat. As shown in Fig. 11, the as-processed BSAS top coat is a two-phase structure composed of the matrix BSAS celsian phase (standard composition 31.5wt% Ba, 4.7% Sr, 15.6% Al, 15.9% Si, and 32.3% O) and another discontinuous, Sr-enriched, "minor" phase with a composition of ~29.7wt% Ba, 13.6% Sr, 18.5% Al, 8.3% Si, and 29.9% O. This phase could not be identified by X-ray diffraction but was crystalline (as determined by electron diffraction.) Since the silica within the BSAS likely contributed to the BSAS volatilization observed during engine testing, less SiO_2 present in the starting and final Sr-rich phases made this a more stable phase. Thus, a key to improving the durability of the top coat for use in this application could be to take advantage of the presence of a Sr-rich phase.

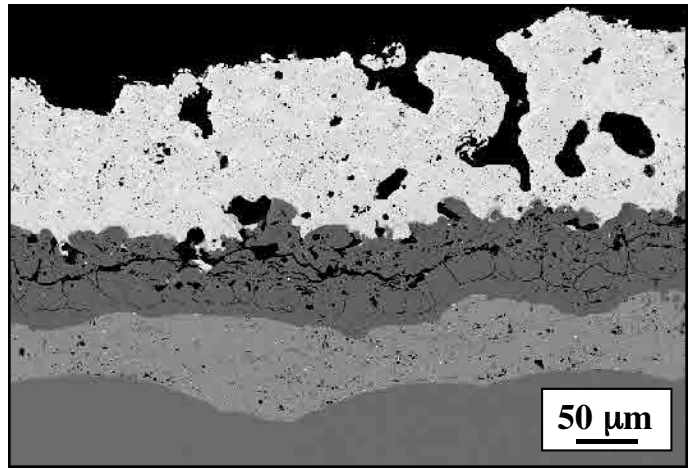


Fig. 8a. SEM image of EBC near aft end of inner liner after engine test (thickness of EBC is close to that of as-processed EBC).

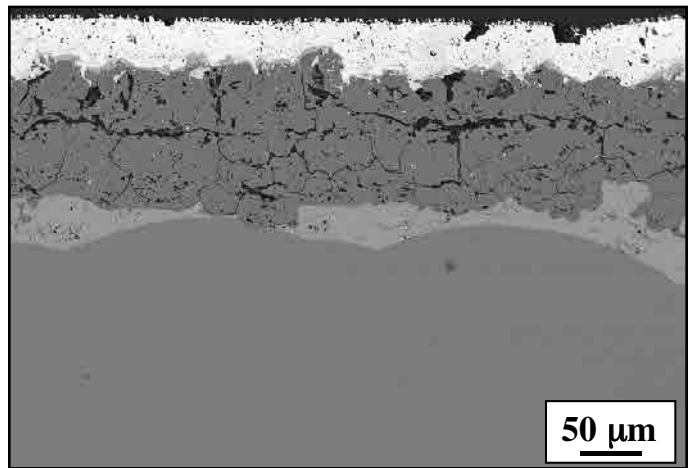


Fig. 8b. SEM image of EBC near center of inner liner after engine testing in an area that appeared to have EBC fully intact but BSAS top coat had recessed to ~75% of its original thickness.

Stability of Mullite in Combustion Environments. In many areas where the BSAS top coat had significantly or completely recessed, the mullite intermediate layer was affected considerably. Once exposed to the combustion environment, the mullite rapidly separated into Al_2O_3 and SiO_2 . The SiO_2 subsequently volatilized leaving behind a porous, completely non-protective layer. This occurred on the inner and outer liner for both the Si/mullite/BSAS and the mixed-layer Si/(mullite+BSAS)/BSAS EBCs. Figure 12 shows an image of the outer liner where the BSAS completely volatilized exposing the mixed intermediate layer (mullite+BSAS) to the combustion environment. The mullite within the mixed layer has started to decompose into SiO_2 and Al_2O_3 (the Al_2O_3 forms around the edges of the mullite, designated by arrows in Fig. 12). The SiO_2 areas have volatilized leaving behind large pores in the layer, rendering the layer non-protective.

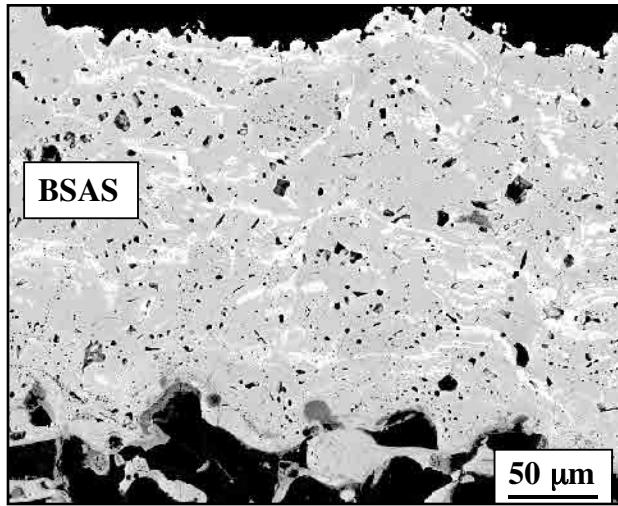


Fig. 9a. SEM image of EBC near aft end of outer liner after engine test (thickness of EBC is close to that of as-processed EBC).

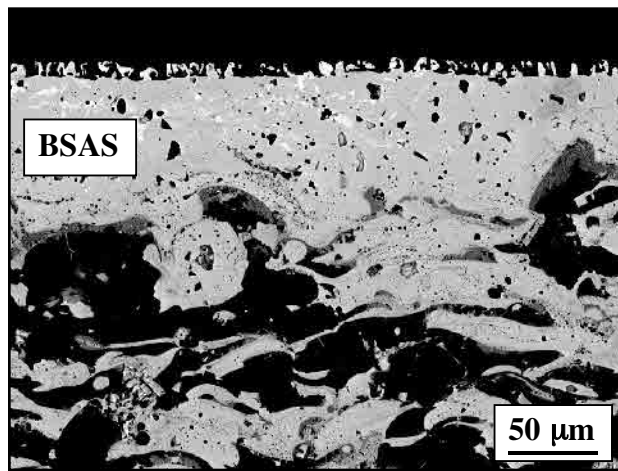


Fig. 9b. SEM image of EBC near center of outer liner after engine testing in an area that appeared to have EBC fully intact but BSAS top coat had recessed to ~60% of its original thickness.

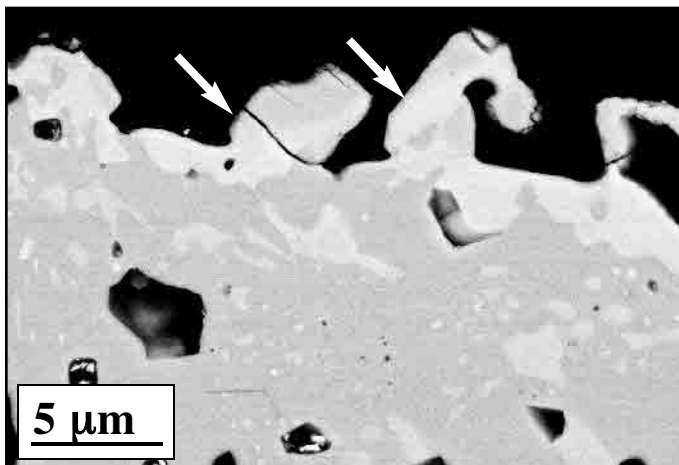


Fig. 10. High magnification image of the surface of a partially volatilized BSAS top coat after engine testing showing $\text{Sr}_2\text{Al}_2\text{SiO}_7$ phase (brightly imaging phase) residing on top coat surface.

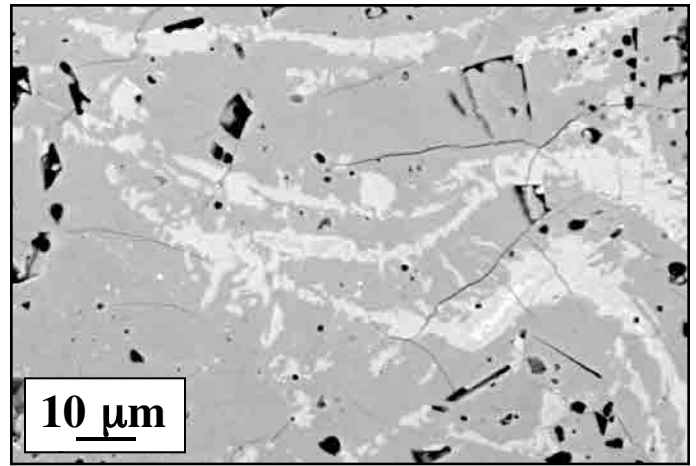


Fig. 11. SEM image of the as-processed BSAS top coat showing a two-phase structure consisting of BSAS (matrix) and a discontinuous Sr-enriched phase (brightly imaging).

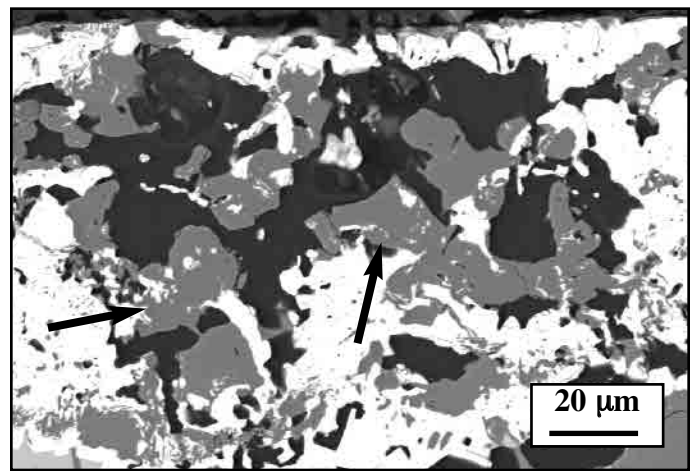


Fig. 12. SEM image of mixed mullite+BSAS layer in an area on outer liner where BSAS top coat had fully recessed during engine testing. Arrows denote pure Al_2O_3 .

Oxidation Of Si Bond Coat Within EBCs. In areas on both the inner and outer liner surfaces where the EBC was fully intact (usually close to the aft or fore ends of liner), oxidation of the Si bond coat was consistently observed. These results were consistent with observations made on similarly processed EBC/CFCC coupons exposed in ORNL's Keiser Rig. Figure 13 shows a region on the inner liner surface near the aft end where the Si/mullite/BSAS standard EBC was intact. Extensive oxidation of the Si bond coat was observed, as evidenced by SiO_2 formation. Associated with these regions were other areas where EBC spallation was observed. Spallation of the BSAS top coat and mullite layer consistently occurred between the SiO_2 layer and mullite intermediate layer (Note separation between these layers in Fig. 13). Figure 14 shows an SEM image of the Si/(mullite+BSAS)/BSAS mixed-layer EBC from the outer liner close to the aft end of the liner. In this case, the EBC imparted greater protection for the underlying constituents and oxidation of the Si bond coat was minimized and was similar to that predicted by Keiser Rig exposures conducted at 1200°C and 1.5 atm H_2O (see Fig. 6).

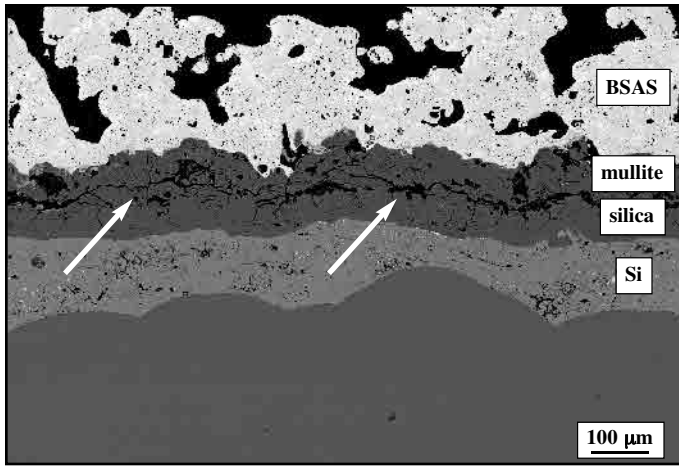


Fig. 13. SEM image of EBC on inner liner near aft end showing extensive oxidation of Si bond coat. Spallation consistently occurs between SiO_2 and mullite (arrows).

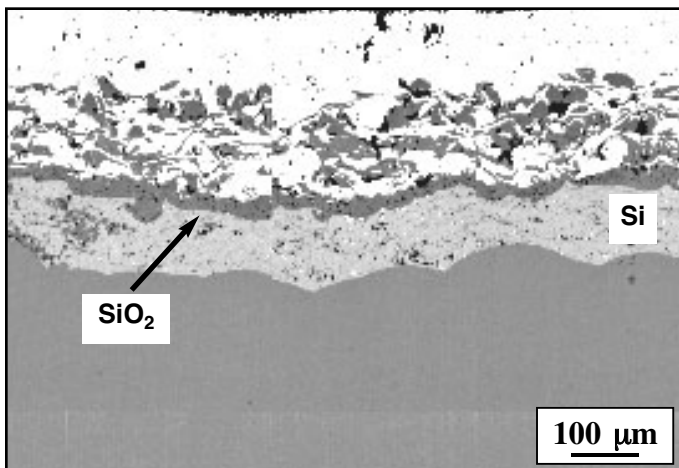


Fig. 14. SEM image of mixed-layer EBC on outer liner near aft end showing minimum oxidation of Si bond coat after ~14,000h engine test consistent with results of Keiser Rig exposures.

Surface Asperities and Pinhole Defect Formation. As shown in Fig. 3c, a regular pattern of “pinhole” defects was observed on the working surfaces of both the inner and outer liners, but was especially prevalent across most of the surface of the outer liner. These defects were initially observed during borescope inspections in the early stages of the engine test and increased in number and severity as the engine test progressed. The spacing of the majority of the defects on the outer liner corresponded directly with the tooling used during the CVI processing of the outer liner. The pattern of “tool bumps” are always observed on the surface of as-processed CVI-produced CFCCs and are caused initially by the slight localized pulling or raising of the wound fibrous preform (usually a single fiber tow) during CVI. The tool bumps on the surface of the liner are still evident following the application of the CVD SiC seal coat, as shown in Fig. 15. The surface asperities at this stage usually measure ~0.2-0.25mm in height. After application of the EBC, the surface asperities are still present, as shown on the surface of an as-processed EBC/CVI-CFCC coupon in Fig. 16. A cross-section directly through a typical tool bump shows that in the

majority of cases, the asperity results in the formation of a through-thickness crack in the EBC, as shown in Fig. 17. Clearly, a through-thickness crack in the EBC will lead to localized accelerated oxidation of the Si bond coat below the surface. In fact, rapid oxidation of the constituents below the surface caused these localized areas to oxidize at rates approaching those of the uncoated CFCCs and severely limited the lifetime of the liner. Figure 18 shows a tool bump area from a relatively cool section (fore end) of the outer liner. In this case, the formation of excessive SiO_2 just below the EBC nearly resulted in the spallation of the EBC. Oxidation did not progress through the CVD SiC seal coat and into the CFCC. However, in much hotter areas near the center of the outer liner, pinholes formed when the rapid oxidation progressed down through the Si bond coat, the CVD SiC, and well into the CFCC, as shown in Fig. 19. In several cases, localized loss of the entire liner thickness resulted from the accelerated oxidation associated with the tool bumps.

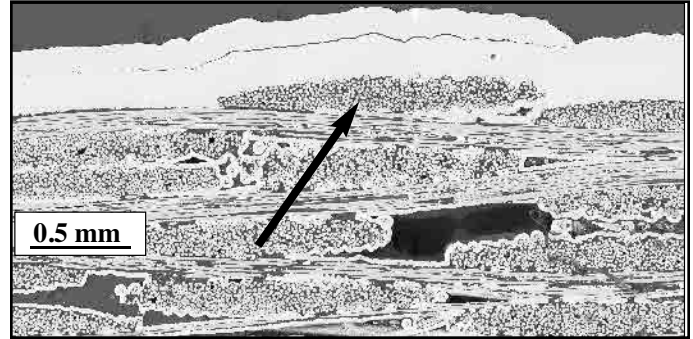


Fig. 15. Cross-section SEM image through a tool-bump after CVD SiC seal coat application. Note raised fiber tow.

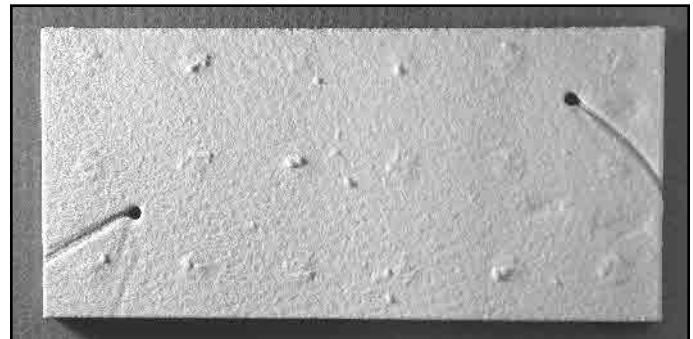


Fig. 16. CVI SiC/SiC coupon after EBC is applied showing obvious surface asperities due to tool bumps.

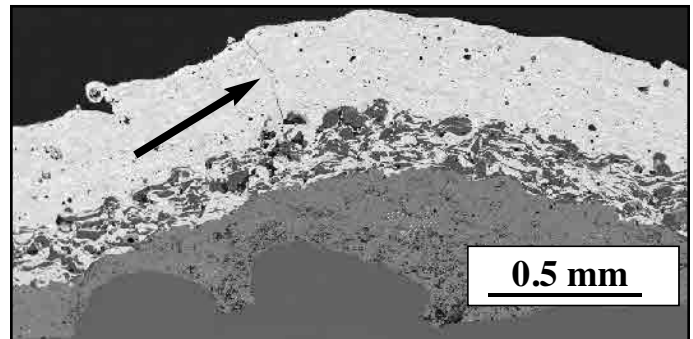


Fig. 17. Cross-section SEM image through a tool bump area showing a through-thickness crack associated with a bump.

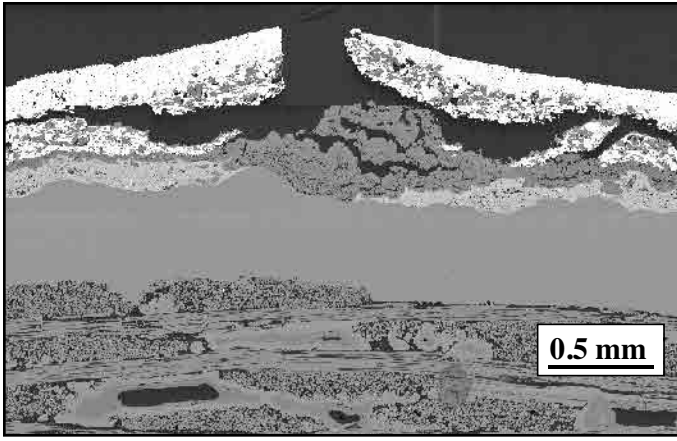


Fig. 18. Cross-section SEM image through a tool bump from fore end (cooler) of outer liner.

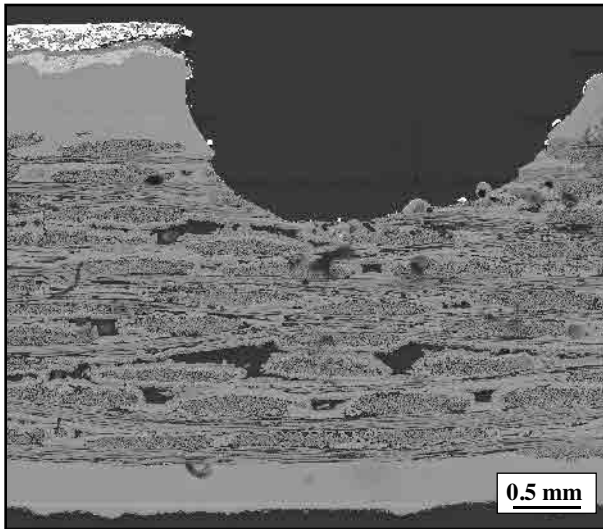


Fig. 19. Cross-section SEM image through a "pinhole" defect formed from a tool bump near center of outer liner.

CONCLUSIONS

The fifth Chevron engine test ran for ~14,000h with EBC/CFCC combustor liners. The EBCs provided additional protection for the CFCC liners compared to CVD SiC seal coated CFCC liners previously engine tested. However, considerable localized EBC damage was observed on the working surface of both the inner and outer liners. Extensive post-test microstructural evaluation of the liners revealed four primary types of EBC degradation that contributed to limiting the liner life: (1) volatilization of BSAS, (2) mullite phase separation and volatilization, (3) sub-surface (Si) oxidation, and (4) surface asperities that caused localized premature EBC spallation and accelerated oxidation. Efforts are currently underway to improve the stability of the BSAS by evaluating improved compositions and to reduce the effect of surface asperities created during the CVI process.

ACKNOWLEDGEMENTS

Research sponsored by the U.S. DOE, Office of Power Technologies, CFCC Program, under Contract DE-AC05-00OR22725 with UT-Battelle, LLC.

REFERENCES

1. Miriyala, N., Simpson, J.F., Parthasarathy, V.J., Brentnall, W.D., 1999, "The Evaluation of CFCC Liners After Field-Engine Testing in a Gas Turbine," ASME Paper 99-GT-392.
2. Miriyala, N. and Price, J.R., 2000, "The Evaluation of CFCC Liners After Field Testing in a Gas Turbine - II," ASME Paper 2000-GT-648.
3. Miriyala, N., Fahme, A., van Roode, M., 2001, "Ceramic Stationary Gas Turbine Program - Combustor Liner Development Summary," ASME Paper 2001-GT-512.
4. More, K.L., Tortorelli, P.F., Ferber, M.K., Keiser, J.R., Miriyala, N., Brentnall, W.D., and Price, J.R., 2000, "Exposure of Ceramics and Ceramic Matrix Composites in Simulated and Actual Combustor Environments," *Journal of Engineering for Gas Turbines and Power*, **122**, pp. 212-18.
5. Ellingson, W.A., Sun, J.G., More, K.L., and Hines, R., 2000, "Non-destructive Characterization of Ceramic Composites Used as Combustor Liners in Advanced Gas Turbines," ASME Paper 2000-GT-68.
6. More, K.L., Tortorelli, P.F., Ferber, M.K., and Keiser, J.R., 2000, "Observations of Accelerated SiC Recession by Oxidation at High Water-Vapor Pressures," *Journal of The American Ceramic Society*, **83**[1], pp. 211-13.
7. More, K.L., Tortorelli, P.F., and Walker, L.R., 2001, "Effects of High Water-Vapor Pressures on the Oxidation of SiC-Based Fiber-Reinforced Composites," *Materials Science Forum*, Vol. **369-372**, pp. 383-94.
8. Opila, E.J. and Hann, R.E., 1997, "Paralinear Oxidation of CVD SiC in Water Vapor," *Journal of The American Ceramic Society*, **80**[1], pp. 197-205.
9. Robinson, R.C. and Smialek, J.L., 1999, "SiC Recession Caused by SiO₂ Scale Volatility Under Combustion Conditions: I, Experimental Results and Empirical Model," *Journal of The American Ceramic Society*, **82**[7], pp. 1817-25.
10. Eaton, H.E., Linsey, G.D., More, K.L., Kimmel, J.B., Price, J.R., and Miriyala, N., 2000, "EBC Protection of SiC/SiC Composites in Gas Turbine Combustion Environment," ASME Paper 2000-GT-631.
11. Eaton, H.E., Linsey, G.D., Sun, E.Y., More, K.L., Kimmel, J.B., Price, J.R., and Miriyala, N., 2001, "EBC Protection of SiC/SiC Composites in the Gas Turbine Combustion Environment - Continuing Evaluation and Refurbishment Considerations," ASME Paper 2001-GT-513.
12. Lee, K.N., 2000, "Current Status of EBCs for Si-Based Ceramics," *Surface Coatings and Technology*, **133-134**, pp. 1-7.
13. Miriyala, N., Kimmel, J.B., Price, J.R., More, K.L., Tortorelli, P.F., Eaton, H.E., Linsey, G.D., and Sun, E.Y., 2002, "The Evaluation of CFCC Liners After Field Testing in a Gas Turbine - III," to be presented at ASME TurboExpo 2002, Amsterdam, The Netherlands, June, 2002 and published as an ASME Paper.
14. Keiser, J.R., Howell, M., Williams, J.J., and Rosenberg, R.A., 1996, "Compatibility of Selected Ceramics with Steam Reformer Environments," *Proceedings of Corrosion/96, NACE International*, Houston, TX, Paper 140.